Nanocrystalline α-MnO_2 Nanowires by Electrochemical Step-Edge Decoration

Qiguang Li,† John B. Olson,‡ and Reginald M. Penner*,†

Department of Chemistry, University of California, Irvine, California 92697-2025, and Boundless Corp., Boulder, Colorado 80301-2747

Received May 6, 2004
Revised Manuscript Received July 8, 2004

α- and γ-MnO_2 are promising candidate materials for cathodes in lithium ion batteries.[1−4] Both of these materials can be converted by electrochemical Li^+ intercalation into the cubic spinel, $Li_{1-x}Mn_2O_4$, which has channels through which Li^+ can move.[2,3] Once the lithiated spinel is formed, the spinel framework of the $Li_{1-x}Mn_2O_4$ cathode is conserved as Li^+ is extracted during discharge and inserted during charging.[5] The kinetics of the Li^+ intercalation reaction coupled with the transport rate for Li^+ in the cathode determines the achievable discharge rates.[6] This fact has motivated an interest in nanometer-scale MnO_2 materials and significant progress has been reported including the synthesis of nanocrystalline MnO_2 films,[7] dispersions of discrete MnO_2 nanoparticles,[8,9] and MnO_2 nanowires, nanorods, and nanofibers.[10−17] 1-D materials are of particular interest because this morphology simultaneously minimizes the distance over which Li^+ must diffuse during the discharge while providing for electrical continuity.

Here we report a simple, one-step electrodeposition method for preparing nanowires of α-MnO_2 that are extremely long (>100 μm), of a controllable diameter between 40 and 150 nm, and nanocrystalline—composed of ≈15 nm diameter α-MnO_2 grains. MnO_2 nanowires were electrodeposited onto the basal plane of a ZYB-

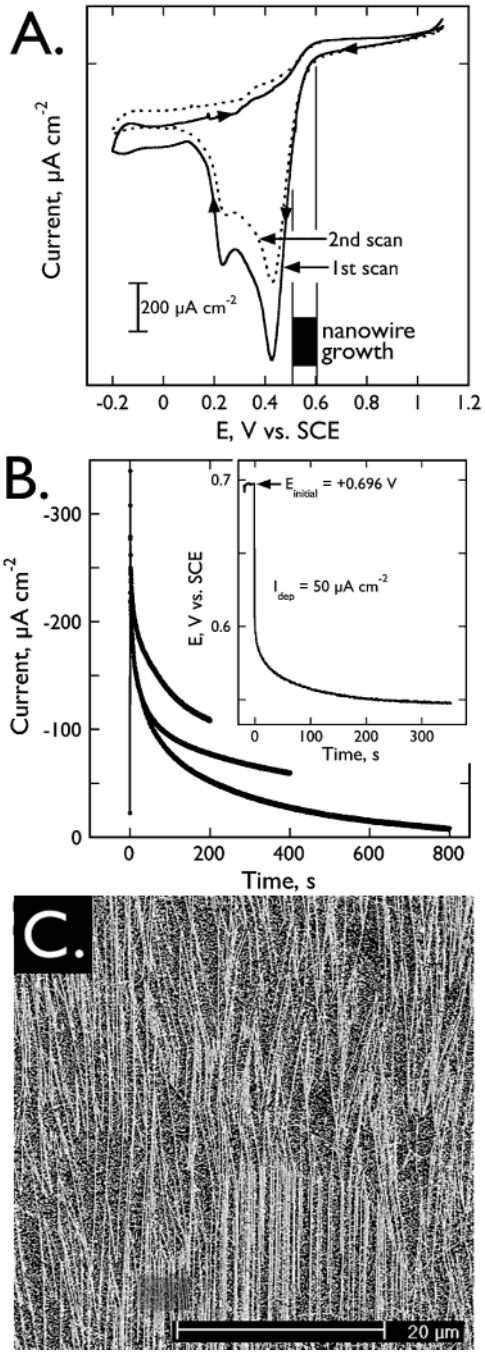

Figure 1. (A) Cyclic voltammograms at 20 mV s^{-1} for an HOPG working electrode in an aqueous plating solution containing 10 mM $KMnO_4$, 0.5 M NaCl, and 0.5 M NH_4Cl at pH 6.5. The black rectangle labeled "nanowire growth" shows the potential range employed for step-edge selective growth of MnO_2 nanowires. (B) Current versus time transients for three MnO_2 electrodepositions at 0.56 V vs SCE with durations of 200, 400, and 800 s. The growth current always decreased as a function of time, but not in proportion to $t^{-1/2}$. (B, inset) Potential vs time curve for the constant current deposition of MnO_2 using a current density of 50 μA cm^{-2}. (C) Representative SEM image of a graphite surface after the deposition of MnO_2 (either potentiostatic or galvanostatic) showing preferential electrodeposition at step edges.

* To whom correspondence should be addressed.
† University of California.
‡ Boundless Corp.

(1) Feng, Q.; Kanoh, H.; Ooi, K. *J. Mater. Chem.* **1999**, *9*, 319−333.
(2) Hill, L. I.; Verbaere, A.; Guyomard, D. *J. Power Sources* **2003**, *119−121*, 226.
(3) Thackeray, M. M. *J. Am. Ceram. Soc.* **1999**, *82*, 3347−3354.
(4) Thackeray, M. M. *Handbook of Battery Materials*; Wiley-VCH: Weinheim, Germany, 1999.
(5) Kim, J. S.; Vaughey, J. T.; Johnson, C. S.; Thackeray, M. M. *J. Electrochem. Soc.* **2003**, *150*, A1498−A1502.
(6) Thackeray, M. M. *Handbook of Battery Materials*,; Wiley-VCH: Weinheim, Germany, 1999.
(7) Moore, G. J.; Portal, R.; La Salle, A. L. G.; Guyomard, D. *J. Power Sources* **2001**, *97−8*, 393−397.
(8) Omomo, Y.; Sasaki, T.; Wang, L. Z.; Watanabe, M. *J. Am. Chem. Soc.* **2003**, *125*, 3568−3575.
(9) Wang, L. Z.; Omomo, Y.; Sakai, N.; Fukuda, K.; Nakai, I.; Ebina, Y.; Takada, K.; Watanabe, M.; Sasaki, T. *Chem. Mater.* **2003**, *15*, 2873−2878.
(10) Xiao, T. D.; Strutt, P. R.; Benaissa, M.; Chen, H.; Kear, B. H. *Nanostruct. Mater.* **1998**, *10*, 1051−1061.
(11) Wu, C. Z.; Xie, Y.; Wang, D.; Yang, J.; Li, T. W. *J. Phys. Chem.* **2003**, *107*, 13583−13587.
(12) Wang, X.; Li, Y. D. *Chem. Lett.* **2004**, *33*, 48−49.
(13) Wang, X.; Li, Y. D. *Chem.-Eur. J.* **2003**, *9*, 300−306.
(14) Wang, X.; Li, Y. D. *J. Am. Chem. Soc.* **2002**, *124*, 2880−2881.
(15) Wang, X.; Li, Y. D. *Chem. Commun.* **2002**, 764−765.
(16) Nishizawa, M.; Mukai, K.; Kuwabata, S.; Martin, C. R.; Yoneyama, H. *J. Electrochem. Soc.* **1997**, *144*, 1923−1927.
(17) Sugantha, M.; Ramakrishnan, P. A.; Hermann, A. M.; Warmsingh, C. P.; Ginley, D. S. *Int. J. Hydrogen Energy* **2003**, *28*, 597.

10.1021/cm049285v CCC: $27.50
Published on Web 08/03/2004

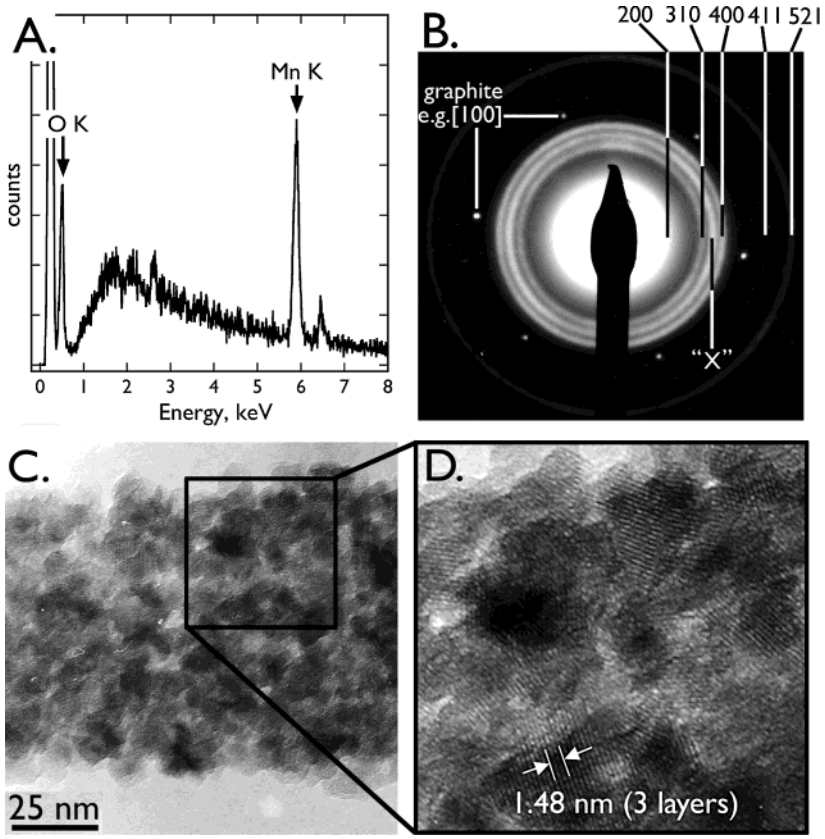

Figure 2. (A) Energy-dispersive X-ray (EDX) spectrum of MnO_2 nanowires showing the presence of Mn and O. (B) Selected area electron diffraction (SAED) patterns of a MnO_2 film prepared at $E_{dep} = 0.56$ V vs SCE from the plating solution indicated in Figure 1A. The indicated diffraction assignments are for α-MnO_2 (JCPDS file 72-1982). One diffraction ring, labeled "X" and corresponding to a *d* spacing of 2.82 Å, cannot be assigned to α-MnO_2. Single-crystal diffraction from the graphite surface is also observed from the equivalent planes [100], [010], etc., with a *d* spacing of 2.13 Å. (C) and (D) Low- and high-magnification TEM images of a 78 nm diameter MnO_2 nanowire. The MnO_2 layer spacing is 4.93 Å and the nanocrystalline grain size is 10−15 nm.

grade HOPG crystal using the electrochemical step edge decoration (ESED) method.[18−22] Briefly, ESED involves the step-edge selective electrodeposition of materials (chiefly metals and metal oxides) on HOPG. Previously, we have demonstrated that MoO_2 nanowires[23,24] can be prepared by electrodeposition at low overpotentials. Figure 1A shows a cyclic voltammogram (CV) at the HOPG basal plane for an aqueous solution containing MnO_4^-. Two reduction peaks were observed, with the most positive of these corresponding to electrodeposition of MnO_2:

$$MnO_4^- + 2H_2O + 3e^- \rightarrow MnO_2 + 4OH^- \qquad (1)$$

Step-edge selectivity was achieved in the electrodeposition of MnO_2 by employing a small overpotential, $\eta <$ |100 mV|, for electrodeposition corresponding to the potential range indicated in Figure 1A. α-MnO_2 was obtained after annealing as-deposited MnO_2 in N_2 at 250−300 °C for 12−24 h. During potentiostatic nanowire growth, the rate of the MnO_2 electrodeposition reaction decreased as a function of time, as shown in Figure 1B, and this is probably a consequence of increasing ohmic resistance through the hemicylindrical nanowire as its radius increases.

The step-edge selective electrodeposition of MnO_2 nanowires can also be realized by constant-current deposition. The inset of Figure 1B shows the potential vs time curve obtained during electrodeposition of MnO_2 at a constant current density of 50 μA cm^{-2}. A negative excursion of the potential from 0.60 to 0.54 V is observed during this 300 s deposition. As seen in Figure 1A, this potential range coincides with potentials where MnO_2 nanowires were obtained in potentiostatic growth experiments.

The graphite basal plane is subdivided by grain boundaries into 0.5−1 mm diameter single-crystal domains. Within the confines of a particular grain, step edges are approximately straight and oriented parallel to one another. The electrodeposition of MnO_2 at these steps therefore produced nanowires that are approximately straight, and up to 1 mm in length, as shown in the low-magnification scanning electron micrograph (SEM) of Figure 1C.

The elemental composition of MnO_2 nanowires was probed using energy-dispersive X-ray spectroscopy (EDX) and a typical result is shown in Figure 2A. EDX spectra indicated the presence of manganese at 5.9 keV and

(18) Zach, M. P.; Ng, K. H.; Penner, R. M. *Science* **2000**, *290*, 2120−2123.
(19) Penner, R. M. *J. Phys. Chem. B* **2002**, *106*, 3339−3353.
(20) Walter, E. C.; Murray, B. J.; Favier, F.; Penner, R. M. *Adv. Mater.* **2003**, *15*, 396−399.
(21) Walter, E. C.; Murray, B. J.; Favier, F.; Kaltenpoth, G.; Grunze, M.; Penner, R. M. *J. Phys. Chem. B* **2002**, *106*, 11407−11411.
(22) Favier, F.; Walter, E. C.; Zach, M. P.; Benter, T.; Penner, R. M. *Science* **2001**, *293*, 2227−2231.
(23) Zach, M. P.; Inazu, K.; Ng, K. H.; Hemminger, J. C.; Penner, R. M. *Chem. Mater.* **2002**, *14*, 3206−3216.
(24) Li, Q.; Newberg, J. T.; Walter, E. C.; Hemminger, J. C.; Penner, R. M. *Nano Lett.* **2004**, *4*, 277−281.

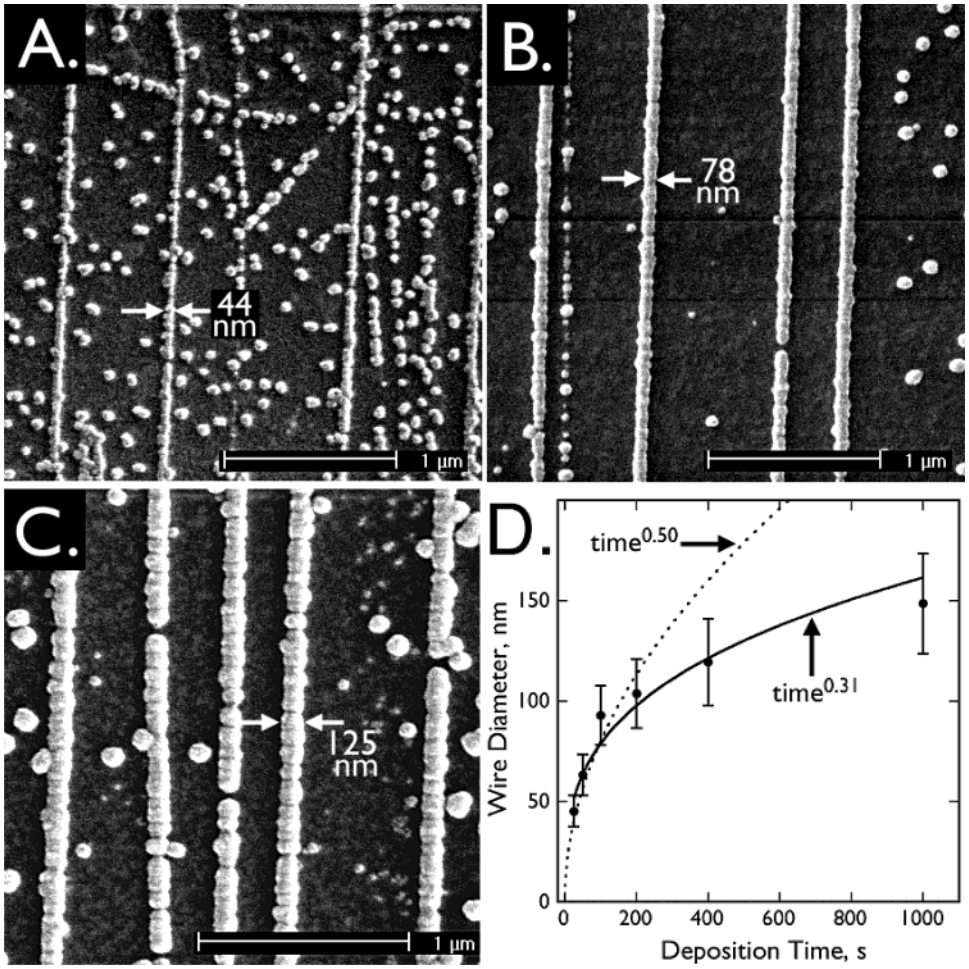

Figure 3. (A−C) SEM images of MnO_2 nanowires prepared at $E_{dep} = 0.58$ V vs SCE for (A) 25 s, (B) 75 s, and (C) 400 s. (D) Plot of mean nanowire diameter (as measured by SEM) as a function of the deposition time. The dashed line shows a fit of the short time diameter data to a time$^{0.50}$ growth law expected for constant current growth of hemicylindrical wires. The best fit to the growth law is obtained using a time$^{0.31}$ growth law (solid line). Error bars indicate $\pm 1\sigma$ in the diameter distribution.

oxygen at 0.53 keV while other elements were absent. The spatial coincidence of the manganese and oxygen EDX signals in the nanowires present on the surface implies that these nanowires are composed of a manganese oxide. Neither X-ray nor electron diffraction could be used directly to characterize MnO_2 nanowires prepared by ESED because the quantity of material was too small. However, with continuation of MnO_2 growth until wires coalesced into films, high-quality SAED powder patterns, such as that shown in Figure 2B, were obtained. As with MnO_2 nanowires, these films were annealed at 300 °C for 24 h. In the SAED pattern of Figure 2B, six diffraction rings are observed and, of these, five can be assigned to α-MnO_2 (JCPDS file 72-1982) as indicated. One diffraction ring, labeled "X" at $d = 2.82$ Å, did not derive from α-MnO_2. The identity of this impurity cannot be known with certainty, but it is most likely Mn_5O_8 (310) with $d = 2.828$ Å or MnO(OH) (301) with $d = 2.8025$Å. The graphite diffraction spots prove that the SAED powder pattern of Figure 2B was collected from the MnO_2 deposited within the confines of a single graphite crystallite. The radial uniformity of the diffraction rings is evidence that the crystallographic orientation of α-MnO_2 grains is not influenced by the atomic structure of the graphite surface.

The internal structure of a 78 nm diameter MnO_2 wire is revealed in the TEM image of Figure 2C. This image shows MnO_2 nanocrystallites with diameters in the 10−15 nm range. At higher magnification (Figure 2D), a lattice spacing of 4.93 Å is obtained—consistent with the (200) lattice spacing of α-MnO_2. Approximately 5% of these nanocrystallites show a lattice spacing of 2.8 Å (data not shown)—close to that expected for the periodicity responsible for the diffraction labeled "X" in Figure 2B. The TEM data suggest that these impurity nanocrystallites are distributed evenly throughout each α-MnO_2 nanowire.

The diameter of the MnO_2 nanowires prepared by ESED can be controlled using the electrodeposition time, t_{dep}. Shown in Figure 3A−C are high-magnification SEM images of MnO_2 nanowires prepared using t_{dep} values in the range from 25 to 1000 s. MnO_2 nanowires with mean diameters in the range from 40 to 150 nm were obtained over the range of t_{dep} values. Because the electrodeposition of MnO_2 occurs at a slow rate near kinetic control, the concentration of MnO_4^- at the surface of each growing nanowire is close to the bulk concentration and no depletion layer is present. Previously,[25−27] we have shown that these "slow-growth"

(25) Penner, R. M. *J. Phys. Chem. B* **2001**, *105*, 8672−8678.
(26) Liu, H.; Penner, R. M. *J. Phys. Chem. B* **2000**, *104*, 9131−9139.

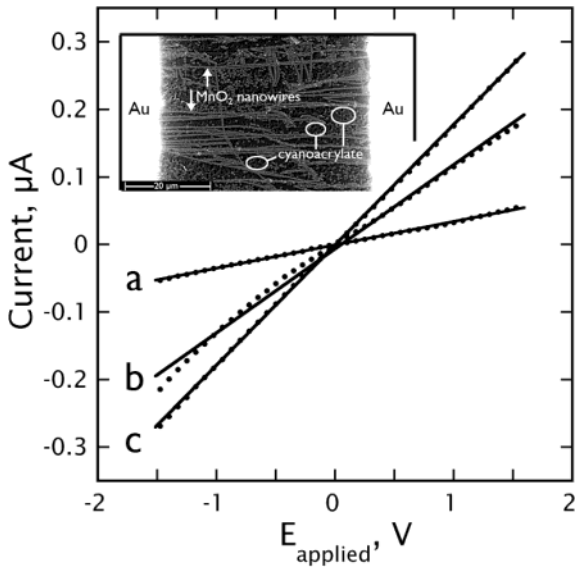

Figure 4. Current versus voltage curves for three ensembles of MnO_2 nanowires after transfer to a cyanoacrylate-coated glass slide and the evaporation of gold contact pads. The resistance obtained from the slopes of these traces are (a) 29 MΩ, (b) 8.1 MΩ, and (c) 5.6 MΩ. Inset: SEM image of an ensemble of transferred MnO_2 wires with a mean wire diameter of 200 nm.

conditions cause the growth rate for each electrodeposited nanostructure on the surface to be independent of its proximity to other nanostructures, leading to a narrow size distribution. For the MnO_2 nanowires prepared here, the relative standard deviation of the nanowire diameter was 15−20%. In prior work involving MoO_2,[23] copper, silver, nickel, and gold[21] nanowires, we found that the wire diameter increased in proportion to $t_{dep}^{1/2}$. This proportionality is expected if the deposition current, i_{dep}, is independent of time, and the nanowire geometry is hemicylindrical. As shown in Figure 2D, the observed increase in MnO_2 wire diameter was well approximated by a much weaker $t_{dep}^{0.31}$ growth law. Qualitatively, this negative deviation from the $t_{dep}^{1/2}$ growth behavior is expected because i_{dep} is not constant during MnO_2 deposition, but decays as a function of time (see Figure 1B).

The utility of these MnO_2 nanowires as battery electrode materials will be limited if they are not electrically continuous. Although we are unable to directly measure the electrical conductance of individual nanowires, the electrical conductivity of ensembles of 10−100 MnO_2 nanowires was measured by transferring MnO_2 wires (after drying in N_2 at 250−300 °C for 12−24 h) from the HOPG surface to cyanoacrylate-coated glass using a previously described procedure.[28] Gold contacts were then evaporated at the ends of these wire ensembles as shown in the inset of Figure 4. These transferred wire ensembles (Figure 4, inset) were characterized by current versus voltage curves that were close to ohmic (Figure 4). This experiment provides evidence for the existence of at least one MnO_2 nanowire that is electrically continuous across a 50 μm gap between the evaporated gold electrodes, and it permits the calculation of an upper limit for the conductivity of the MnO_2 present in these wires of 0.1−1.0 Ω^{-1} cm^{-1}.

In summary, the ESED method can be used to synthesis α-MnO_2 nanowires that are very long (> 100 μm), are of a controllable diameter ranging from 40 to 150 nm, and are nanocrystalline.

Experimental Procedures. *MnO_2 Nanowire Deposition.* MnO_2 nanowires were electrodeposited from unstirred, N_2 purged, aqueous plating solutions having the following composition: 1.0−10 mM $KMnO_4$ (Fisher-certified ACS grade), 0.50 M NaCl (Fisher-certified ACS grade), and 0.50 M NH_4Cl (J. T. Baker) adjusted to pH to 6.5−7.5 using ammonium hydroxide (Fisher ACS grade). The basal plane of a highly oriented pyrolytic graphite (HOPG) crystal was used as the working electrode in a three-electrode cell. All electrochemical measurements were performed using a computer-controlled EG&G 2263 potentiostat. After nanowire growth was complete, the HOPG electrode was washed with Nanopure water (ρ > 18 MΩ) and blown dry using filtered, compressed air. As-deposited MnO_2 nanowires were annealed in N_2 at 250−300 °C for 12−24 h in a sealed quartz tube.

Electron Microscopy and Electron Diffraction. Scanning electron microscopy (SEM) was performed using a Philips FEG-30XL microscope using an accelerating voltage of 10−25 keV equipped with an EDX elemental analyzer. Transmission electron microscopy (TEM) was carried out on a Philips CM-20 using an accelerating voltage of 200 keV. The area analyzed in SAED measurements was 2.5 μm in diameter.

Acknowledgment. This work was funded by the U.S. Department of Energy (Grant DE-FG02-03ER-83614). We are grateful to Dr. Art Moore, formerly of GE Advanced Ceramics Inc., for donations of graphite.

CM049285V

(27) Liu, H.; Favier, F.; Ng, K.; Zach, M. P.; Penner, R. M. *Electrochim. Acta* **2001**, *47*, 671−677.

(28) Walter, E. C.; Favier, F.; Penner, R. M. *Anal. Chem.* **2002**, *74*, 1546−1553.